

Supplementary

Peptide-Induced Self-Assembly of Therapeutics into a Well-Defined Nanoshell with Tumor-Triggered Shape and Charge Switch

Wangxiao He^{†,‡,§}, Jin Yan^{//,⊥}, Wei Jiang[‡], Shichao Li[†], Yiping Qu[‡], Fan Niu^{†,§}, Yuwei Yan[†],
Fang Sui[‡], Simeng Wang[‡], Yi Zhou[#], Liang Jin[#], Yujun Li[‡], Meiju Ji⁺, Peter X Ma^{//},
Min Liu[#], Wuyuan Lu[§], Peng Hou[‡]

[†] Center for Translational Medicine, Key Laboratory of Biomedical Information Engineering of Ministry of Education, School of Life Science and Technology, Xi'an Jiaotong University, Xi'an 710049, China.

[‡] Key Laboratory for Tumor Precision Medicine of Shaanxi Province and Department of Endocrinology, The First Affiliated Hospital of Xi'an Jiaotong University, Xi'an 710061, China

[§] Institute of Human Virology and Department of Biochemistry and Molecular Biology, University of Maryland School of Medicine, Baltimore, MD 21201, USA.

^{//} Department of Biologic and Materials Sciences, Department of Biomedical Engineering, Macromolecular Science and Engineering Center, Department of Materials Science and Engineering, University of Michigan, Ann Arbor, Michigan 48109, USA

[⊥] Frontier Institute of Science and Technology, State Key Laboratory for Mechanical Behavior of Materials, Xi'an Jiaotong University, Xi'an 710049, China

[#] Department of Infectious Diseases, The First Affiliated Hospital of Xi'an Jiaotong University , Xi'an 710061, China

⁺ Center for Translational Medicine, The First Affiliated Hospital of Xi'an Jiaotong University, Xi'an 710061, China

Supplementary Catalogue

Supplementary Catalogue	1
Supplementary Methods	4
General remarks.....	4
Synthesis of peptide (PSP molecules and ^D PMI).	4
CD spectroscopy.....	4
Transmission Electron Microscopy (TEM).	4
Cell culture and cell viability analysis.....	5
Western blot analysis.	5
Apoptosis and cell cycle analysis.....	6
Immunohistochemical (IHC) staining.	7
Safety Evaluation.	7
Supplementary Figures	9
Figure S1. Design and characterization of the self-assembled peptides.	9
Figure S2. pH-responsive charge reversal and size switches of Molecule #11 and 12.....	10
Figure S3. The effect of concentration of PSP-DPMI on self-assembled structure.	11
Figure S4. pH-responsive charge reversal and size switches of PSP-(L) ^D PMI. 12	
Figure S5. Stability of PSP- ^D PMI in cell culture medium including 20% human serum.....	13
Figure S6. The cellular uptakes of the FITC-labeled PSP- ^D PMI into the normal	

cells.....	14
Figure S7. Average radiance of the Ex vivo fluorescence intensity in tumors and major organs	15
Figure S8. Pharmacokinetic study after intravenous injection.....	16
Figure S9. <i>Ex vivo</i> fluorescent images of tumors and major organs from PSP-DPMI ^{FITC} -treated mice at different time after intravenous injection.....	17
Figure S10. The integrin expression IN HCT116, MCF7 and A375 cells.....	18
Figure S11. The p53 expression levels in A375 and MCF7 cells.....	19
Figure S12. Apoptosis analysis in HCT116 p53+/+ cells treated with PSP-DPMI.	20
Figure S13. Cell cycle analysis in HCT116 p53+/+ cells treated with PSP-DPMI.	21
Figure S14. The body weight of the mice with different treatments.	22
Figure S15. Toxicity evaluation of the spleen in mice with the indicated treatments.	23
Figure S16. Toxicity evaluation of the heart in mice with different treatments...	24
Figure S17. The content of hemoglobin and eosinophils.	25
Figure S18. Toxicity evaluation of the lung in mice with the indicated treatments.	26

Supplementary Methods

GENERAL REMARKS.

All synthetic peptide sources were obtained from CS Bio (Shanghai) Ltd. All other chemicals used in this study were purchased from Sigma-Aldrich unless otherwise specified. Acetonitrile and water (HPLC grade) were purchased from Fisher Scientific Ltd. All products were used as received without further purification.

Synthesis of peptide (PSP molecules and ^DPMI).

All peptides were synthesized on appropriate resins on an CS bio 336X automated peptide synthesizer using the optimized HBTU activation/DIEA in situ neutralization protocol developed by an HBTU/HOBt protocol for Fmoc-chemistry SPPS.⁶⁴ After cleavage and deprotection in a reagent cocktail containing 88% TFA, 5% phenol, 5% H₂O and 2% TIPS, crude products were precipitated with cold ether and purified to homogeneity by preparative C18 reversed-phase HPLC. The molecular masses were ascertained by electrospray ionization mass spectrometry (ESI-MS).

CD SPECTROSCOPY.

CD spectra of Lupbin variants at a concentration of 20 μM in 10 mM phosphate buffer (pH 7.4) were obtained at room temperature on a J-810 spectropolarimeter (Jasco, Easton, MD) using a 1-mm quartz cuvette. Scanned area was from 250 nm to 190 nm, and the scanning speed was 50 nm/min. Every curve was the average of three independent detections.

TRANSMISSION ELECTRON MICROSCOPY (TEM).

To image dried PSP or PSP-^DPMI –shells, 1 μ L of concentrated hollow shells solution was deposited on TEM grids. TEM analysis was carried out with a Tecnai F30 transmission electron microscope operating at 120 kV. Elemental analysis at a line across the shells was performed in scanning TEM (STEM) mode using an EDAX X-ray detector.

CELL CULTURE AND CELL VIABILITY ANALYSIS.

Human colon cancer cell line HCT116 p53^{+/+} (wild-type p53) was purchased from ATCC and maintained in McCoy's 5A medium with 10% FBS. The isogenic HCT116 p53^{-/-} (p53 deletion) cells were presented by Prof. Bert Vogelstein of Johns Hopkins University (Baltimore, MD), and maintained in McCoy's 5A medium with 10% FBS. Melanoma cell line A375 and breast cancer cell line MCF7 were also purchased by ATCC and maintained in DMEM with 10% FBS. Cells were plated in 96-well plates at a density of 2500 cells/well (100 μ L). After 24 h, cells were treated with PSP-^DPMI, PSP, ^DPMI and Nutlin3 at the indicated concentrations and times, respectively. All samples were settled by twice echelon dilution from 20 μ M to 5 nM. The *in vitro* cytotoxicity was then measured by using a standard MTT (Thermo Fisher scientific) assay. Of note, 2 mM HEPES-HCL were used to adjust the pH of cell culture medium to 6.5.

WESTERN BLOT ANALYSIS.

Cells were treated with PSP-^DPMI (200 nM), PSP (200 nM), ^DPMI (200 nM) and Nutlin3 (5 μ M) for 24 h, respectively. Cells were then lysed in prechilled RIPA buffer containing protease inhibitors, and equal amounts of protein lysates were separated by 10% SDS-PAGE and transferred onto PVDF membranes (Roche Diagnostics, Mannheim, Germany). The membranes

were subsequently incubated with the indicated primary antibodies at 4°C overnight. Antibodies against p53 and p21 were purchased from Abcam (p53: ab131442, 1:500 dilutions; p21: ab109199, 1:1000 dilutions). Antibody against β -actin was purchased from Sigma-Aldrich (A5441, 1:5000 dilutions). This was followed by incubation with their respective HRP-conjugated secondary antibodies from Calbiochem, and immunoblotting signals were visualized using the Western Bright ECL detection system (Advansta, CA).

APOPTOSIS AND CELL CYCLE ANALYSIS.

Necrosis/apoptosis was evaluated by flow cytometric analysis using the FITC Annexin V Apoptosis Detection Kit (BD Biosciences). Briefly, cells were treated with PSP-^DPMI (200 nM), PSP (200 nM), ^DPMI (200 nM) or Nutlin3 (5 μ M) for 48 h. Cells were then harvested, washed twice with cold PBS, and re-suspended in 1 \times binding buffer at a concentration of 1×10^6 cells/mL. One hundred microliters of the solution (1×10^5 cells) was transferred to a 5mL culture tube, followed by addition of 5 μ l of FITC Annexin V and 5 μ L of PI. After gentle vortexing and a 15-min incubation in the dark at room temperature, 400 μ L of 1 \times binding buffer was added to the tube, and cells were analyzed by FACS.

For cell cycle analysis, cells were first serum starved for 12 h, and then treated with PSP-^DPMI (200 nM), PSP (200 nM), ^DPMI (200 nM) or Nutlin3 (5 μ M) for 24 h. Next, cells were harvested, washed twice in PBS, and fixed in 70% ethanol on ice for at least 30 min. After that, cells were stained with propidium iodide (PI) solution (50 μ g/ml PI, 50 μ g/mL RNase A, 0.1% Triton-X, 0.1 mM EDTA). Cell cycle distributions were then analyzed based on DNA contents by a flow cytometer (BD Biosciences, NJ).

IMMUNOHISTOCHEMICAL (IHC) STAINING.

Sections were cut at 5 μm thickness, deparaffinized and rehydrated. Endogenous peroxidase activity was blocked with hydrogen peroxide/methanol, and antigen retrieval was performed in a pH 9.0 TE (Tris-EDTA) buffer by autoclave for 10 min. The resultant tissue sections were then incubated with the antibodies against p53 (Abcam), p21 (Abcam) and Ki67 (Abcam) at 4°C overnight. After incubation with labeled streptavidin-biotin (LSAB) complex for 15 min, the slides were stained and visualized by using the iView DAB detection system (ZSGB-BIO, P.R. China). Each stained section was evaluated by a minimum of 10 randomly selected $\times 20$ high-power fields for further statistical analysis.

To evaluate immunostaining intensity (I), we used a numeric score ranging from 0 to 3, reflecting the intensity as follows: 0, no staining; 1, weak staining; 2, moderate staining; and 3, strong staining. To evaluate immunostaining area (A), we used a numeric score ranging from 1 to 4, reflecting the intensity as follows: 1, positive area <10%; 2, 10%<positive area <50%; 3, 50%<positive area <90%; and 4, positive area >90%. Using an Excel spreadsheet, the mean score was obtained by multiplying the intensity score (I) by the percentage of positive area and the results were added together (total score: $I \times A$).

SAFETY EVALUATION.

To measure potential *in vivo* safety hazard of repeatedly infusing PSP-^DPMI, we monitored body weight of all mice over the course of treatment and measured hematological indexes as well as organ function indexes after a 13-day treatment (same as the treatment in the section of evaluation

of *in vivo* antitumor activity). Control mice were only implanted with xenograft tumor but did not receive any treatment. Healthy mice without any treatment were used as normal control. At the end of the treatment, mice were anesthetized, and blood was immediately collected for complete blood count (CBC) determinations, including a white blood cell count with differential, a red blood cell count, haemoglobin and a platelet count. Blood was also collected into serum separator tubes for serum chemistry and cytokine profile analyses (performed by Clinical Laboratory at The First Affiliated Hospital of Xi'an Jiaotong University). Besides, blood serum was collected, and mouse alanine aminotransferase (ALT), aspartate transaminase (AST), blood urea nitrogen (UN) and creatinine (CRE) were measured by using quantitative enzyme-linked immunosorbent assay (ELISA) kits, following validation of each ELISA kit according to the manufacturer's instructions. Animals were then euthanized with carbon dioxide to retrieve organs, which were washed with deionized water before fixation in 4% paraformaldehyde. The tissues were processed routinely, and sections were stained with haematoxilin and eosin (H&E).

Supplementary Figures

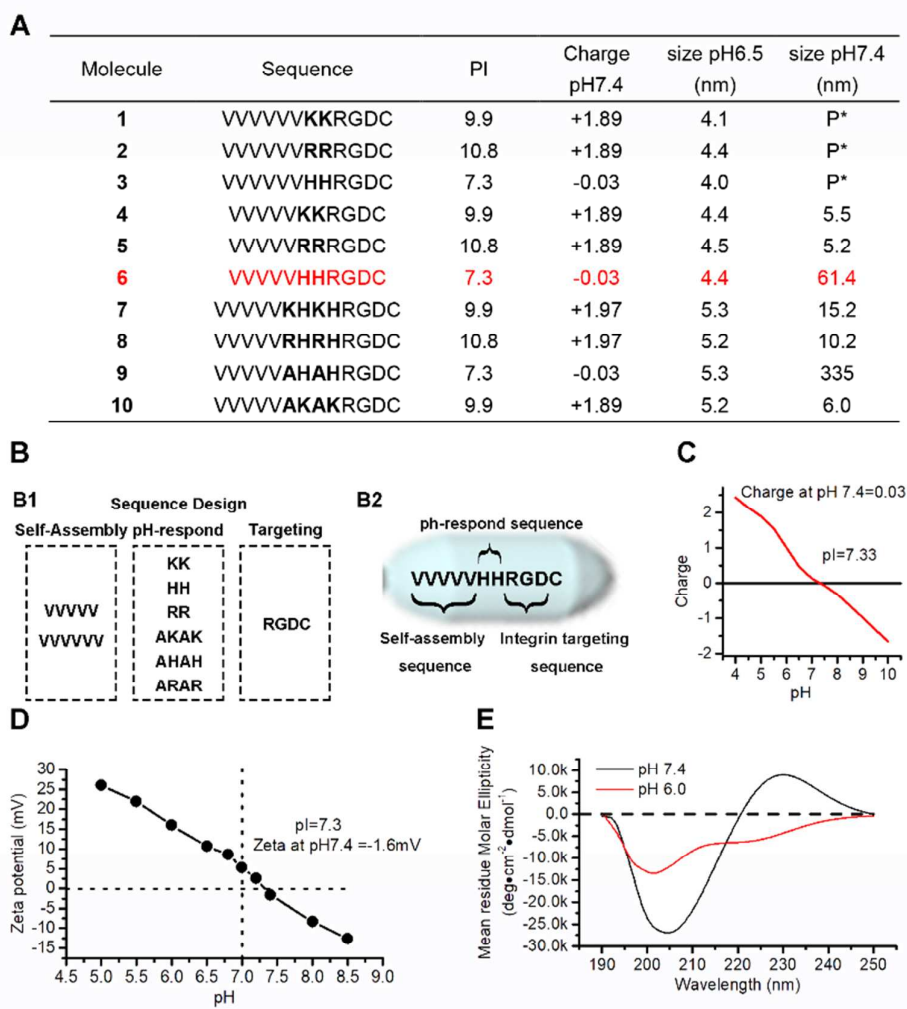


FIGURE S1. DESIGN AND CHARACTERIZATION OF THE SELF-ASSEMBLED PEPTIDES. (A) List of peptide-amphiphile tails. PI (isoelectric point) and charge pH 7.4 were calculated by PROTEIN CALCULATOR (<http://protcalc.sourceforge.net/>). Sizes were the hydrodynamic size at pH 7.4 and pH 6.5, which were measured by dynamic light scattering (DLS) 30 mins after pH adjustment. P* stands for precipitate, whose hydrodynamic size was more than 10 μ m. All the polydispersity index (PDI) of the DLS samples were lower than 0.2. (B) Schematic illustration of self-assembly peptide-amphiphile tails. (B1) The sequence illustration of peptide-amphiphile tails consisting of three parts. (B2) The sequence illustration of molecular #6. (C) The charges of molecular #6 from pH 4 to 10, which were also calculated by PROTEIN CALCULATOR. (D) Zeta potential of PSP in PBS buffer (10 mM) at different pH, suggesting that the Charge characteristics of the PSP was accordant with the theoretical values by PROTEIN CALCULATOR in (C). (E) CD spectrum of PSP in PBS at pH6.0 or 7.4. At pH 7.4, the negative characteristic absorption peak at 205 indicated the β -sheet formation.

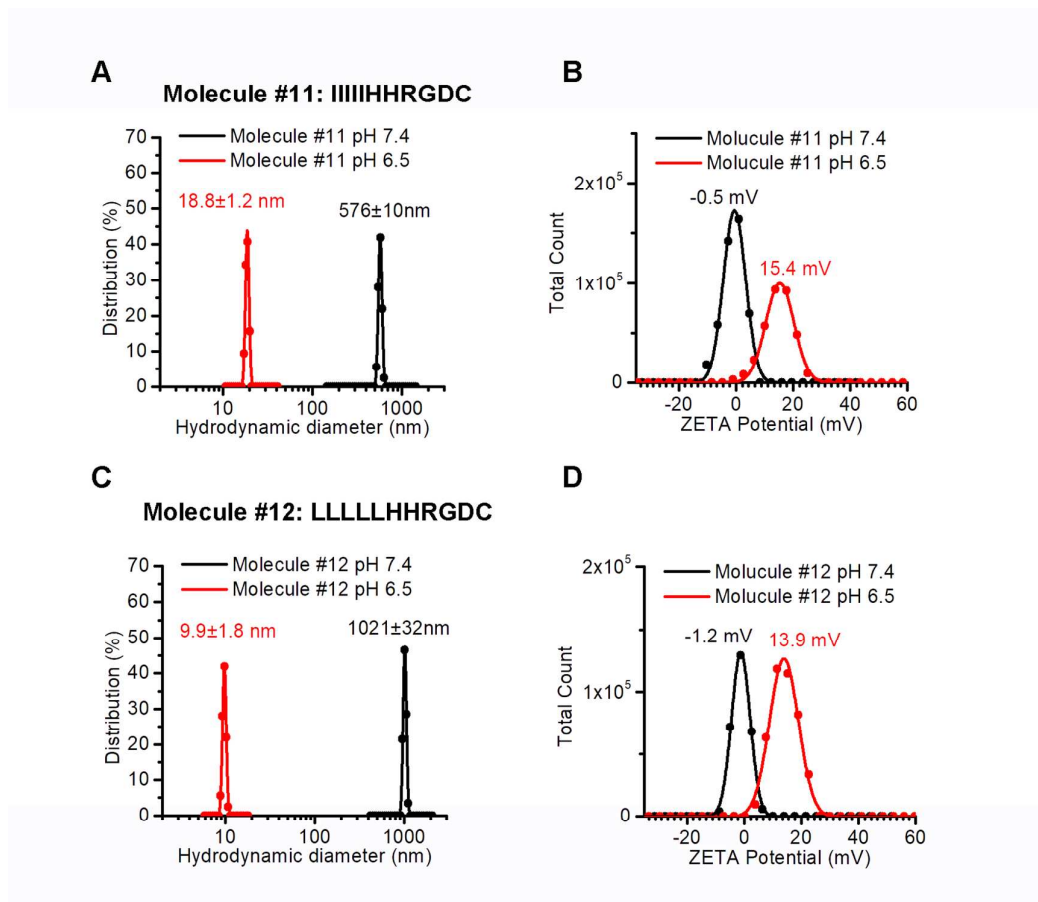


FIGURE S2. PH-RESPONSIVE CHARGE REVERSAL AND SIZE SWITCHES OF MOLECULE #11 AND 12. The size (A) and surface charge (zeta potential) (B) of molecule #11 (at pH 7.4 and pH 6.5), which were measured at 37 °C in aqueous solution. The size (C) and surface charge (zeta potential) (D) of molecule #12 (at pH 7.4 and pH 6.5)

Concentration (mg/ml)	Size at pH7.4	PDI
1.6	1054	0.650
0.8	695	0.230
0.4	365	0.202
0.2	61.4	0.167
0.1	60.6	0.120
0.05	59.8	0.101

FIGURE S3. THE EFFECT OF CONCENTRATION OF PSP-DPMI ON SELF-ASSEMBLED STRUCTURE. The size was the hydrate particle size measured by DLS in PBS buffer at 37°C.

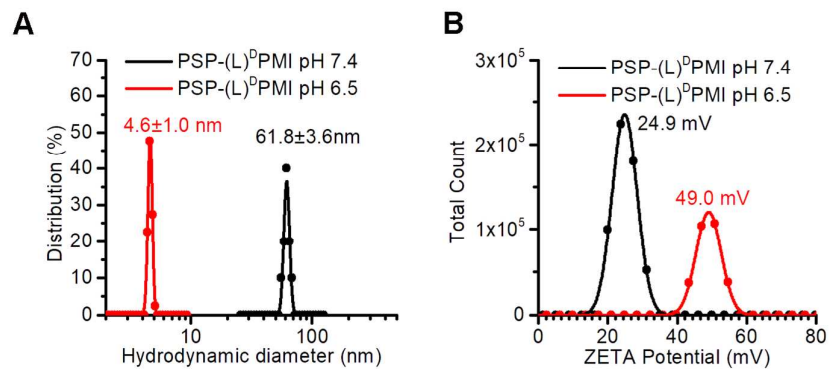


FIGURE S4. PH-RESPONSIVE CHARGE REVERSAL AND SIZE SWITCHES OF PSP-(L)^DPMI. The size (A) and surface charge (zeta potential) (B) of PSP-(L)^DPMI (at pH 7.4 and pH 6.5), which were measured at 37 °C in PBS solution. (L)^DPMI is the L-isomeride of the ^DPMI.

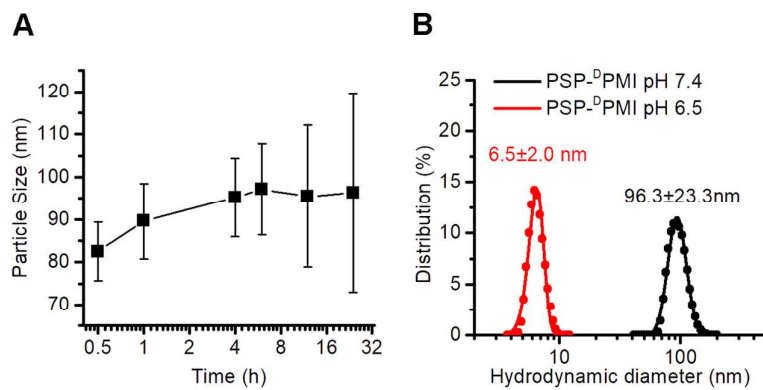


FIGURE S5. STABILITY OF PSP-DPMI IN CELL CULTURE MEDIUM INCLUDING 20% HUMAN SERUM. (A) The size of the PSP-DPMI during the incubations with DMEM medium containing 20% human serum. The size (B) of PSP-DPMI (at pH 7.4 and pH 6.5), which were measured by DLS after a 24-h incubation with DMEM medium containing 20% human serum. Human serum was purchased from Sigma-Aldrich (SLBR5973V).

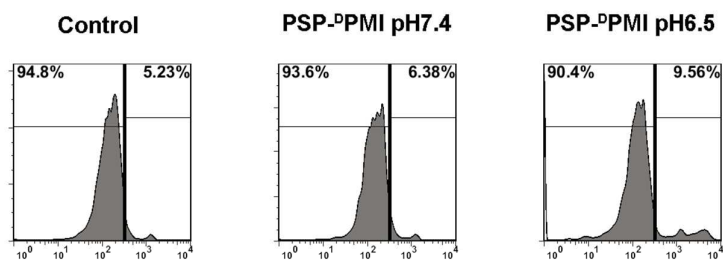


FIGURE S6. THE CELLULAR UPTAKES OF THE FITC-LABELED PSP-DPMI INTO THE NORMAL CELLS. The normal cells (non-cancerous cells) used here were the peripheral blood mononuclear cells (PBMC) separated from blood of health C57 mice. The cellular uptakes of the FITC-labeled PSP-DPMI were measured by flow cytometry after a 6-h incubation with 20 $\mu\text{g/mL}$ PSP-DPMI^{FITC} at pH 7.4 or pH 6.5.

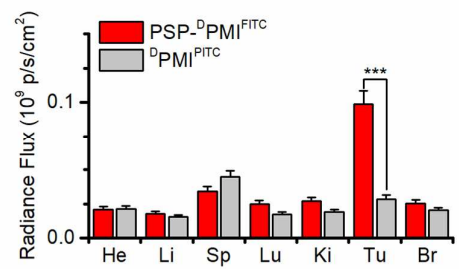


FIGURE S7. AVERAGE RADIANCE OF THE EX VIVO FLUORESCENCE INTENSITY IN TUMORS AND MAJOR ORGANS. Every tissue was exposed at same exciting light and normalize by the PBS control group. All data were shown by mean±s.d. (n =3/group). He, heart; Li, liver; Sp, spleen; Lu, lung; Ki, kidneys; Tu, tumor; Br, Brain.

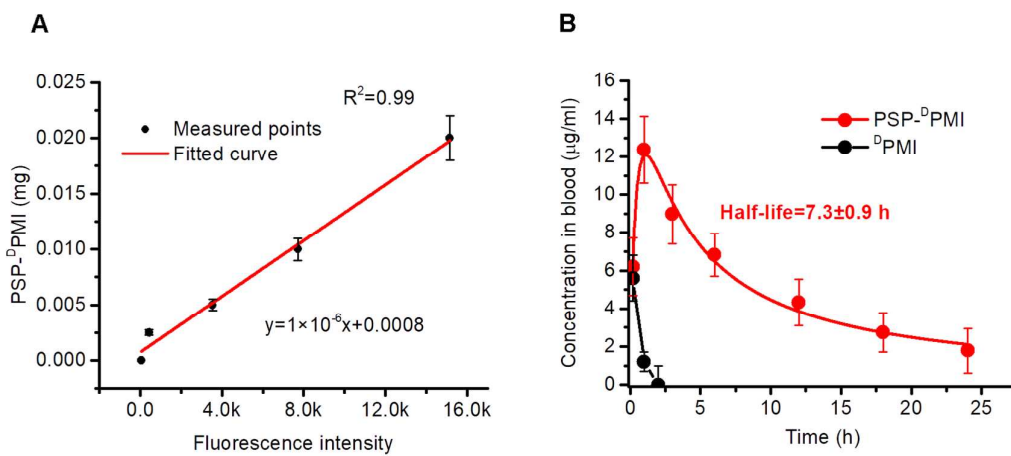


FIGURE S8. PHARMACOKINETIC STUDY AFTER INTRAVENOUS INJECTION. (A) Standard curve of the concentration of the FITC-labeled PSP-^DPMI and the fluorescent intensity. The FITC-labeled PSP-^DPMI was solved in mice blood to measure the standard curve. (B) The Pharmacokinetic results of the FITC-labeled PSP-^DPMI and FITC-labeled ^DPMI. The half-life of the PSP-^DPMI was 7.3 h, where ^DPMI can not be found after 2 h.

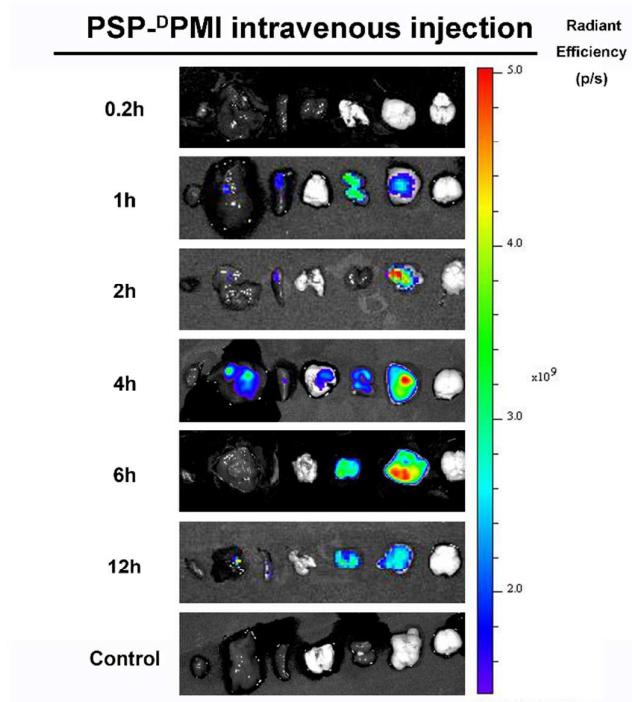


FIGURE S9. *EX VIVO* FLUORESCENT IMAGES OF TUMORS AND MAJOR ORGANS FROM PSP-^DPMI^{FITC}-TREATED MICE AT DIFFERENT TIME AFTER INTRAVENOUS INJECTION. Organs order from left to right were heart, liver, spleen, lung, kidneys, tumor and brain. Thresholds were appropriately established: 1.0×10^9 .

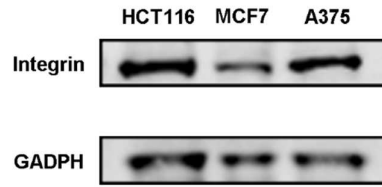


FIGURE S10. THE INTEGRIN EXPRESSION IN HCT116, MCF7 AND A375 CELLS.
GAPDH was used as control.

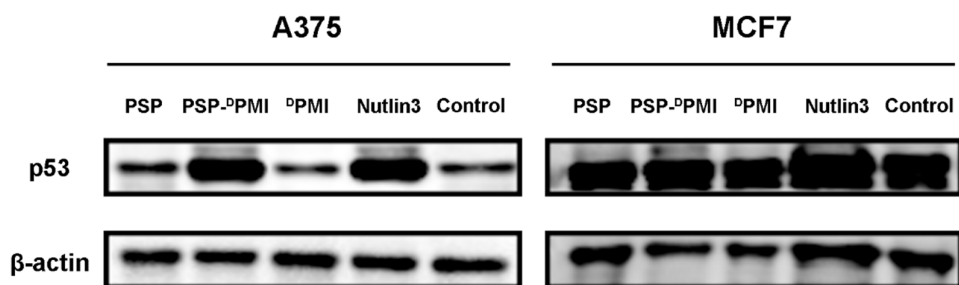


FIGURE S11. THE P53 EXPRESSION LEVELS IN A375 AND MCF7 CELLS. Cells were treated with PSP (200 nM), ^DPMI (200 nM), PSP-^DPMI (200 nM) and Nutlin3 (5 μM) for 24 h, and western blot analysis was performed to analyze the expression of p53 proteins. β-actin was used as loading control.

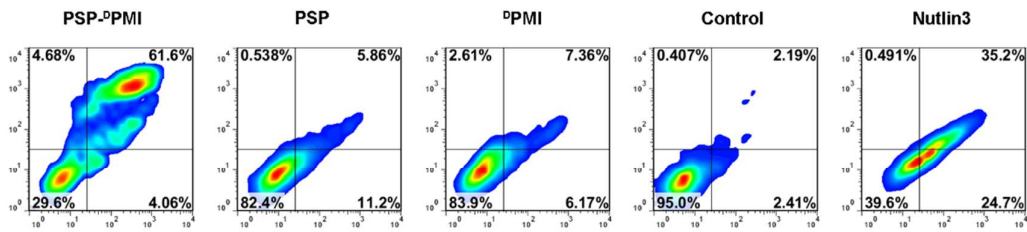


FIGURE S12. APOPTOSIS ANALYSIS IN HCT116 P53^{+/+} CELLS TREATED WITH PSP-^DPMI. HCT116 p53^{+/+} cells were treated with 0.2 μM PSP-^DPMI, 0.2 μM PSP, 0.2 μM ^DPMI, 5 μM Nutlin-3 or isometric PBS for 48 h, and cell apoptosis was then evaluated by flow cytometry using the Annexin V-FITC/PI Apoptosis Detection Kit (abscissa: Annexin V; ordinate: PI).

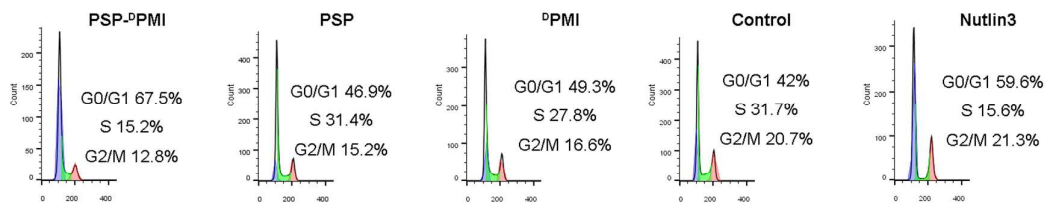


FIGURE S13. CELL CYCLE ANALYSIS IN HCT116 P53^{+/+} CELLS TREATED WITH PSP-DPMI. HCT116 p53^{+/+} cells were treated with 0.2 μ M PSP-DPMI, 0.2 μ M PSP, 0.2 μ M DPMI, 5 μ M Nutlin-3 or blank control for 24 h, and cell cycle distributions were then analyzed by flow cytometry.

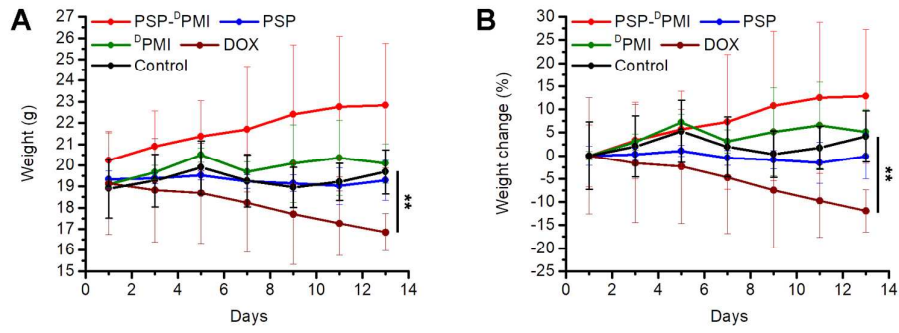


FIGURE S14. THE BODY WEIGHT OF THE MICE WITH DIFFERENT TREATMENTS. The time course of body weight (**A**) and body weight change (**B**) of mice with the indicated treatments. Data were presented as mean \pm s.e. ($n = 5$). Statistically significant differences were indicated: **, $p < 0.01$.

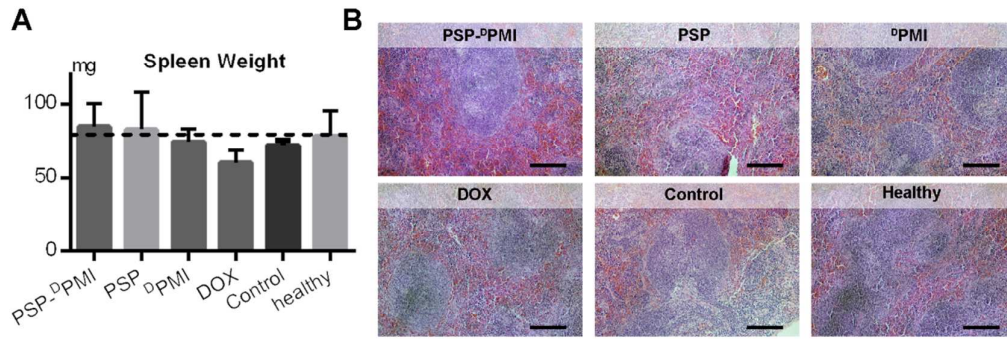


FIGURE S15. TOXICITY EVALUATION OF THE SPLEEN IN MICE WITH THE INDICATED TREATMENTS. (A) Spleen weight of mice with the indicated treatments. Data were presented as mean \pm s.e. (n =5). (B) The representative H&E staining of spleen sections in mice with the indicated treatments ($\times 200$). Scale bar: 50 μ m.

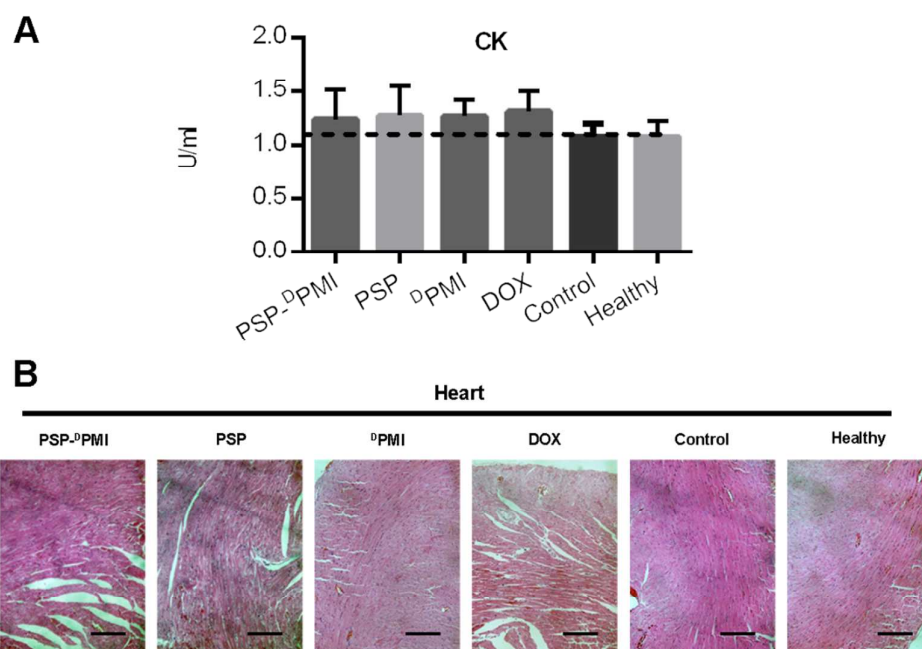


FIGURE S16. TOXICITY EVALUATION OF THE HEART IN MICE WITH DIFFERENT TREATMENTS. (A) CK Serum creatine kinase (CK) activity of mice with the indicated treatments. Clinically, CK is assayed in blood tests as a marker of damage of CK-rich tissues such as in myocardial infarction (heart attack). **(B)** The representative H&E staining of heart sections in mice with the indicated treatments ($\times 200$). Scale bar: 50 μm .

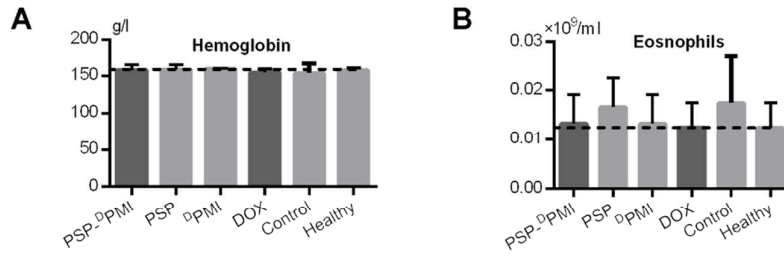


FIGURE S17. THE CONTENT OF HEMOGLOBIN AND EOSINOPHILS. The content of hemoglobin (**A**) and the count of eosnophils (**B**) in the blood of mice with the indicated treatments. Data were presented as mean \pm s.e. (n =5).

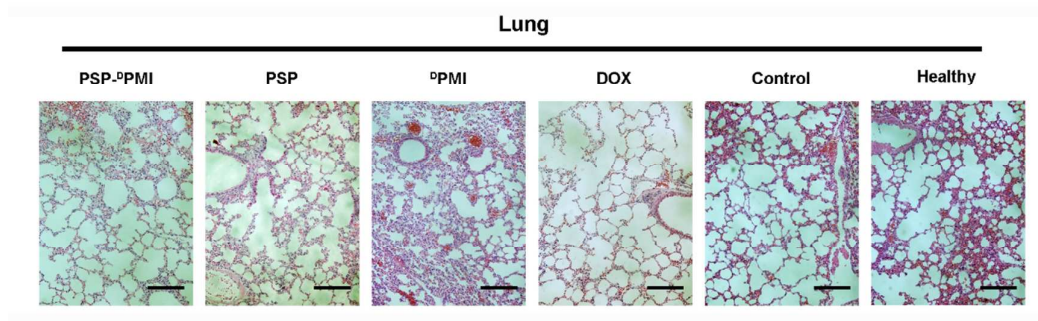


FIGURE S18. TOXICITY EVALUATION OF THE LUNG IN MICE WITH THE INDICATED TREATMENTS. The representative H&E staining of lung sections in mice with the indicated treatments ($\times 200$). Scale bar: 50 μm .